International Journal of Advanced Geosciences, 6 (1) (2018) 1-13

International Journal of Advanced Geosciences

Website: www.sciencepubco.com/index.php/IJAG
doi: 10.14419/ijag.v6i1.8573
Research paper

Basement Classification through Enhanced Magnetic Data Reductions in parts of Ekiti State, Southwestern Nigeria

Akingboye A. S.[1] *, Ogunyele A. C. [1]

[1] *Department of Earth Sciences, Adekunle Ajasin University, Akungba-Akoko, PMB 001, Ondo State, Nigeria*
**Corresponding Author E-mail: adedibu.akingboye@aaua.edu.ng*

Abstract

Enhanced magnetic data reductions via the use of various forms of filters were employed for basement classification in parts of Ekiti State. The data reductions and enhancement involve: reduction to equator (RTE), regional and residual, automatic gain control (AGC), downward continuation, upward continuations (1, 2, and 3 km), analytic signal (AS) and horizontal gradient (HG) to map and delineate basement rocks and structures, while surface relief and spectral plot were used to determine depth to top of magnetic sources. The images revealed that the study area is characterized by different lithologies. The rocks evinced lineaments and faults trending NE-SW (G–G', H–H', J–J', K–K'), NNE-SSW, E-W (minor) and approximately N-S, while the dykes are in NW-SE, NNW-SSW directions. The analytic signal (AS) and horizontal gradient (HG) revealed high amplitude reversed Z-like shape as migmatite rocks, differentiating them from the two flanks with low amplitude signals as schist and quartzite schist of Ijero and Aramoko and the granitic intrusive within these migmatised rocks around Ijan, Gbonyin and Ise/Otun. The shaded relief and the spectral plot showed that the total depth to top of magnetic sources ranged from 20m to 1.8km for shallower and deeper sources respectively.

Keywords: *Magnetic Reductions; Filtering; Basement; Structures; Depth.*

1. Introduction

It is important for magnetic data to be properly filtered by application of various reductions, in order to derive much information from the dataset which are used for both qualitative and quantitative interpretations as well as to accentuate important diagnostic features or anomalies. Filtering techniques are most effective when dealing with shallow source depths, as well as for lithogical and structural mapping. The variations in mineral compositions, chemical inhomogeneities, depositional and/or crystallization conditions and post deformational conditions, play a vital role in geological and structural interpretations.

Magnetic method has been researched by various authors in areas of data processing (reductions and data enhancement) and robust interpretations for various applications, most especially in classifying the subsurface and mapping of geological structures for solid mineral and hydrocarbon explorations, groundwater study, environmental/pollution study, etc have been made.

Automatic gain control (AGC) converts waveforms of variable amplitude into waveforms of semi-constant amplitude in magnetic data. The net result is the removal of amplitude information from data sets, producing a representation of the data that gives an equal emphasis to signals with both low and high amplitudes (Milligan and Gunn, 1997). AGC stacked profiles (Rajagopalan, 1987; Mudge, 1991) and images (Rajagopalan and Milligan, 1995) are extremely useful for structural mapping because they tend to show coherent alignments not apparent in true amplitude data.

More also, analytic signal has been utilized widely for mapping of structures and for determining the depth of sources. The analytic signal (Nabighian, 1972; Roest et al., 1992) and the enhanced analytic signal (Hsu et al., 1996, 1998) were applied to detect the edge and depth estimation of magnetic bodies. Ansari and Alamdar, (2009) showed that analytic signal or total gradient is formed through the combination of the horizontal and vertical gradients of the magnetic anomaly, and it is applied either in space or frequency domain, generating a maximum directly over discrete bodies as well as their edges. The generated maximum directly over the causative body and depth estimation abilities of this filter make it a highly useful technique for magnetic data interpretation. The maximum can be used to detect the structures responsible for the observed magnetic anomalies over an area. Jeng et al. (2003) showed that, the advantage of this magnetic data enhancement method is that its amplitude function is always positive and does not need any assumption about the direction of body magnetization.

Analytic signal maps/images are useful as a type of reduction to the pole, as they are not subjected to the instability that occurs in transformations of magnetic fields from low magnetic latitudes (MacLeod et al., 1993); source positions regardless of any remanence in the sources (Milligan and Gunn, 1997).

Information on the depth and other geometrical source parameters are provided by radially averaged power spectrum (spectral plot). The derived parameters serve as an important basis for providing information that becomes a guide for the subsequent exploration processes, such as drilling and ore body modeling (Okubo, et al.,

Copyright © 2018 Akingboye A. S., Ogunyele A. C. This is an open access article distributed under the Creative Commons Attribution License, which permits unrestricted use, distribution, and reproduction in any medium, provided the original work is properly cited.

2003; Abraham et al., 2014; Okpoli and Akingboye, 2016a, 2016b).

Once the main field and the minor source effects are removed from the observed magnetic field data through the use of these data reductions and processing techniques, the data are then enhanced and presented for interpretation. Copious amounts of significant geologic information such as structure, lithology, alteration, regolith/overburden and sedimentary processes, among other factors are deduced (Luyendyk, 1997; Milligan and Gunn, 1997; Gunn et al., 1997; Mackey et al., 2000).

The geological ingredients that can be interpreted from magnetic surveys are those that influence the spatial distribution, volume and concentration of the magnetically significant minerals. It is important to realize that the magnetic data serve only as an indicator because it is generally impossible to ascertain a definitive, unambiguous and direct lithological or structural interpretation (Ross, 2002).

Therefore, this research is aimed at classifying the basement in parts of Ekiti State using magnetic data enhancement and reductions to map and delineate basement rocks, structures, anomaly closures, edges and boundaries and depth of magnetising bodies.

2. Geologic Setting of the Study Area

Ado-Ekiti, the study area is in Ekiti State, Southwestern Nigeria. It is confined within Latitude 7^0 30' - 8^0 00' N (830000 – 885000 mN) and Longitude 5^0 00' - 5^0 30' E (720000 – 773500 mE) of Zone 31 Greenwich Mercator (Fig. 1). The towns in the study area include Ijero, Aramoko, Ikogosi, Ilawe, Moba, Otun, Ido-osi, Ifaki, Irepodun/Ifelodun, Ado, Ikere, Ise/Otun, Igede, Gbonyin, Ijan and Ikole The study area has prominent rivers, namely; Oyi, Eju, Omo, etc. The areas are accessible, mainly by roads and foot paths.

The study area falls within the Basement Complex of Southwestern Nigeria. The Basement Complex rocks of Nigeria form a part of the African Crystalline Shield which occurs within the Pan-African Mobile Belt that lies between the West African and Congo cartons and South of the Tuareg Shield which were affected by the Pan-African Orogeny. Southwestern Nigerian Basement forms the triangular portion of the Nigerian basement, an extension of the Dahomeyide Shield of the West African Craton. Rocks of the region include Migmatized-Gneiss Complex (MGC) that is characterized by a) grey foliated gneiss, b) ultramafic rocks and c) felsic component comprised of pegmatite, aplite and granitic rocks (Oyawoye, 1972; Rahaman, 1981). The MGC in Southwestern Nigeria is affected by three major geotectonic events ranging from Early Proterozoic of 2000 Ma to Pan-African events of ~600 Ma (Woakes et al., 1987; Ajibade and Fitchews, 1988; Oyinloye, 2011). The rocks from the basement have been affected by medium pressure Barrovian metamorphism (Rahaman et al., 1983; Oyinloye, 2011).

The general geology of the study area is well researched in the works of Rahaman, 1976; Ademilua, 1997; Okunlola et al., 2011; Oyinloye, 2011; Ayodele 2013; Bayowa et al., 2014. The major lithological units include the migmatites, granite gneises, charnockites, granites, granodiorites, schists, schistose quartzite, and other felsic and mafic intrusive (Ademilua, 1997, Oladapo and Ayeni, 2013). The Basement rocks show great variations in grain size and in mineral composition. Migmatisation is widespread throughout the area, often reflected by rapid alternation of granite and biotite gneiss, which grade into one another.

Deformation of the Nigerian Basement Complex occurred in two phases, a ductile phase, which is responsible for the formation of planar structures (foliations and folds) and a brittle phase resulting in jointing and fractures, many of which have been filled with Quartzo-feldspathic veins, dolerite dykes, pegmatite and aplitic veins and dykes (Omosanya et al., 2015). Geological structures such as faults, joints, folds, lineaments, etc. are very common in the migmatite, gneises and schists in the area. The basic geologic structure (folds) of the Southwestern Nigerian Basement Complex is a complementary anticlinorium and synclinorium with northwards plunging axes (Jones and Hockey, 1964; Rahaman, 1974). Consequently, NS, NE-SW, NW-SE, NNE-SSW, NNW-SSE and to a less extent, E-W fractures have developed in these rocks (Oluyide and Udoh 1989; Eze et al., 2011).

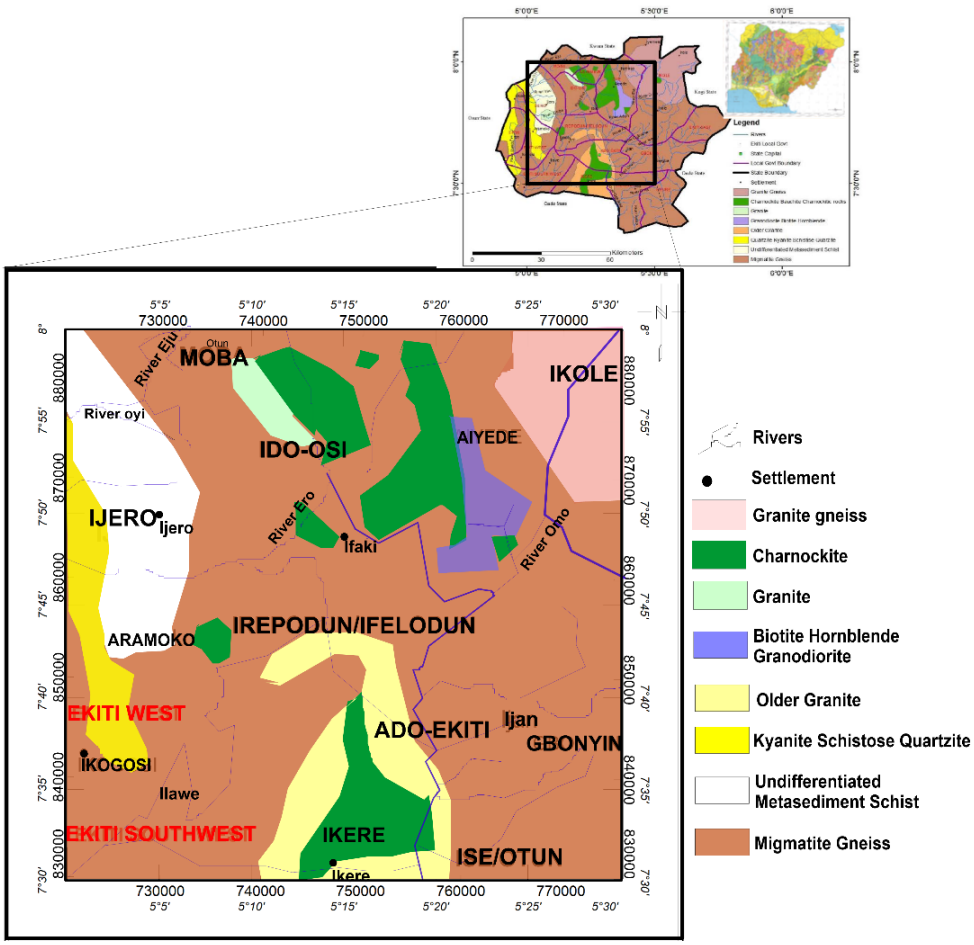

Fig. 1: Geological Map of the Study Area (created from Ademilua, 1997).

3. Material and Methods

Aeromagnetic Sheet 244 data (1:100,000) 000 covering Ado-Ekiti and its environs were acquired from Nigerian Geological Survey Agency (NGSA) and processed using Geosoft® Oasis Montaj™ software. Another software like Surfer and Microsoft Excel was also used in this work.

Data reductions such as; removal of interfering noise, reduction to magnetic equator, regional and residual, downward and upward continuations, automatic gain control, analytic signal, radially averaged power spectrum (spectral plot) etc. were performed on the acquired data. The data reductions and corrections involved the following procedures:

1) The NGSA Total Magnetic Intensity (TMI) data coordinates were re-projected from UTM Zone 32N to UTM Zone 31N of the Greenwich Mercator. This was necessary because the coordinates of the data must correspond to their actual locations.

2) Near Surface Noises (NSN) caused by metallic materials, fences, cables (both buried and surface), flight height and others was the first process to be carried out on the TMI data acquired from NGSA.

3) Reduction to Magnetic Equator (RTE) map was produced by using the RTE filter on the TMI griddled data. This RTE data is then adopted as our new processed data with enhanced signal from the magnetic sources down depth for other filtering processes. To reduce the magnetic data to the equator; equation 2 (Leu, 1981; Montaj^{TM}, 2004) was applied in the data.

$$L(\theta) = \frac{[\sin(I) - i.\cos(I).\cos(D-\theta)]^2 * (-\cos^2(D-\theta))}{[\sin^2(I_a) + \cos^2(I_a).\cos^2(D-\theta)] * [\sin^2(I) + \cos^2(I).\cos^2(D-\theta]}$$
$$\text{if}(|I_a| < |I|), I_a = I \quad (1)$$

where;
$L(\theta)$ = TMI Reduction to Equator (RTE)
I = geomagnetic inclination
I_a = inclination for amplitude correction (never less I)
D = geomagnetic declination

D (°)	I (°)	H (nT)	Z (nT)	F (nT)	X (nT)	Y (nT)
-1.545	-10.385	32717	-5996	33262	32705	-882

4) The Regional Field (data smoothed upward to 4km) associated with deep masses were filtered out to produce the Residual data for the area covered. The data left after near surface noises and the regional effects had been removed using equation 2 is called the Residual.

$$\text{Residual field} = \text{Observed Total field (RTE)} - \text{Regional field} \quad (2)$$

5) Downward continuation is used to enhance features at a specified depth/elevation, lower than the acquisition level. This procedure accentuates near surface anomalies and can be used as an interpretation tool to determine the depth to a causative body by emphasizing shorter wavelengths, but can be unstable and produce artefacts. This is done using equation 3 (MontajTM, 2004):

$$L(r) = e^{hr} \quad (3)$$

h is the distance in meters to be continued downward.

6) Upward Continuation is considered a clean filter because it produces almost no side effects that may require the application of other filters or processes to correct. Because of this, it is often used to remove or minimize the effects of shallow sources and noise in grids. Also, upward continued data may be interpreted numerically and with modeling programs. This is not the case for many other filter processes. Upward continuation was carried out on the RTE data to depth of 1, 2 and 3 km respectively. Equation 4 (Telford et al., 1990) below can be used for the calculation of the upward continuation.

$$F(x,y,-h) = \frac{h}{2\pi}\iint \frac{F(x,y,0)\partial x\partial y}{\{(x-x')^2+(y-y')^2+h^2\}^{1/2}} \qquad (4)$$

Where; $F\,(x',y',-h)$ is the total field at the point $\mathrm{P}\,(\mathrm{x}',\mathrm{y}',-\mathrm{h})$above the surface on which $\mathrm{F}\,(\mathrm{x}',\mathrm{y}',0)$) is known, h is the elevation above surface.

7) The amplitude A of the analytic signal (AS) of the total magnetic field F is calculated from the two or three orthogonal derivatives of the field for 2D or 3D bodies respectively (equations 5; a – c), being defined as the square root of the squared sum of the vertical and horizontal derivatives of the magnetic field (Nabighian, 1972; Roest et al., 1992):

$$\mathrm{A(x,y)} = |\mathrm{A(x,y)}|.\exp(\mathrm{j}\varphi) \qquad (5a)$$

with

$$|\mathrm{A(x,y)}| = \sqrt{\left(\frac{\partial \mathrm{F}}{\partial \mathrm{x}}\right)^2 + \left(\frac{\partial \mathrm{F}}{\partial \mathrm{y}}\right)^2 + \left(\frac{\partial \mathrm{F}}{\partial \mathrm{z}}\right)^2} \qquad (5b)$$

and

$$\varphi = \tan^{-1}\left(\frac{\partial \mathrm{F}}{\partial \mathrm{z}}\middle|\frac{\partial \mathrm{F}}{\partial \mathrm{x}}\right) \qquad (5c)$$

$|\mathrm{A(x,y)}|$ is the analytic signal amplitude, $\varphi$the local phase and Fis the observed magnetic field at (x, y). A common term of the normalized derivatives is the concept of mapping angles (or functions of angles) derived from the gradients of the magnetic intensity.

8) Radially Averaged Power Spectrum (RAPS) was run for depth to magnetic sources estimations. The depth to top of magnetic sourcesis calculated fromthe spectral plot by using equation 6:

$$\mathrm{z} = \frac{\mathrm{m}}{4\pi} \qquad (6)$$

The data reductions and enhancements were done using the MagMap step-by-step filtering processing. Data were griddled from respective reductions for interpretation phase. The gridding method fits minimum curvature curves (which is the smoothest possible surface that would fit the given data values) to data point using method described by Briggs, (1974) and Fitzgerald, et al. (1997). Therefore, various maps produced from all reductions were qualitatively and quantitatively interpreted. The qualitative interpretation was done by inspecting the maps for magnetic variations and signatures (anomalous zones) that are diagnostic of some target points, while the quantitative aspect covers the depth estimation, structural identifications and modeling.

4. Results and Discussion

The shaded colour TMI map (Fig. 2) of the study area is characterized by positive magnetic values ranging from 4.60 to 146.5 nT and negative values from -165.1 to -15.2 nT. High positive magnetic values (100 – 146.5 nT) dominated the close border end of the southwestern part to wide area extent in the central part. Asides the numerous smaller scattered magnetic anomalies at the southern and northern parts, there lies a wide high negative magnetic anomaly (-165 nT) directly above the central positive magnetic anomaly indicating that these areas are highly fractured and weathered. Compared with geological information, the high negative anomalies correlate with the charnockites, granites, granodiorites, and some part of the deformed migmatite gneisses. Quiet zones (27 – 50 nT) indicate areas with slight geological deformation, dominating the extreme NW-SW and ENE-WSW parts (Ilawe, Ikogosi, Aramoko, Ijero, River Oyi, Otun, Gbonyin to eastern part of Ekiti State (Fig. 4)).It is evident from the TMI map that there are different crystalline basement rocks and these areas have been subjected to deformation of varying intensities throughout the geological period resulting to fractures giving way for low rich magnetic bearing minerals and fluid in them.

Reduction to the magnetic equator (RTE) (Fig. 3) is used in low magnetic latitudes to centre the peaks of magnetic anomalies over their sources depending on the inclination and declination of the local field of the magnetizing body. As discussed by Macleod et al. (1993), problems can arise in the reduction to the pole process at magnetic latitudes less than 15°, as the Fourier domain transformation process becomes unstable, owing to the need to divide the spectrum by a very small term, thereby introducing north–south alignment of the anomalies into the data. Besides, the equator passes through Nigeria making the vertical component of the magnetizing field to be almost zero. Therefore, RTE is better considered in this situation for anomalies to lie symmetrically over their exact sources without losing any geophysical meaning.

On comparison with the TMI (Fig. 2), the contoured RTE image shows much more similar features only that anomalies appear to be well defined. The RTE evinces gently trending NW-SE anomalies at the central to northern part and NE-SW trends at the southern part. At the northern part around Ido-Osi to Moba, Aiyede and Ikole complexes (Fig. 4), high-amplitude negative anomalies with highly pronounced structures were revealed.

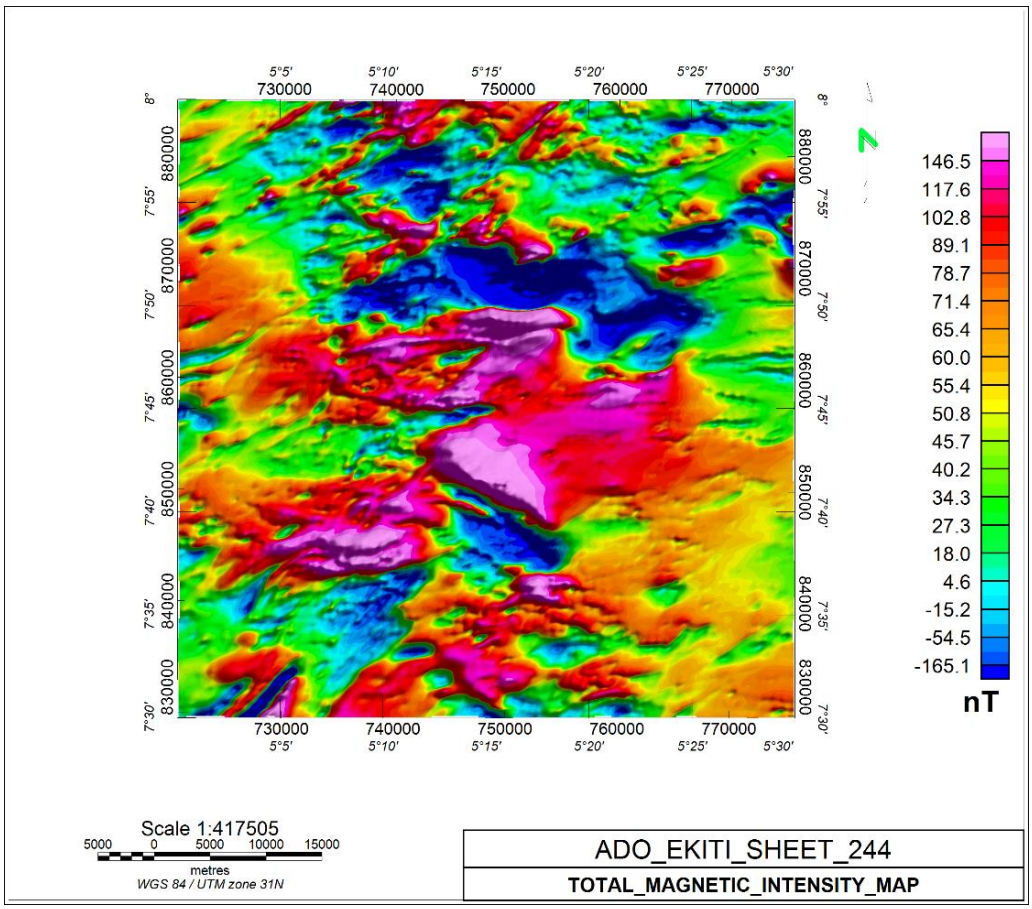

Fig. 2: Colour Shaded Total Magnetic Intensity (TMI) Map.

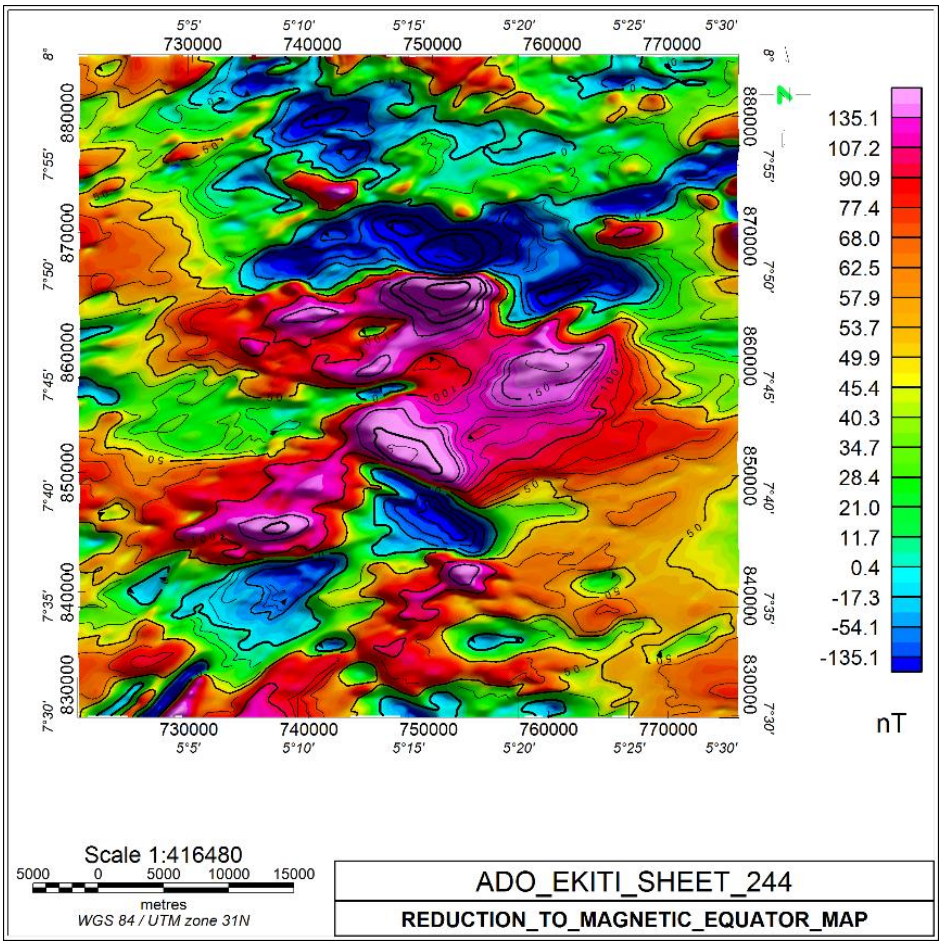

Fig. 3: Contoured Reduction to Magnetic Equator (RTE) Map.

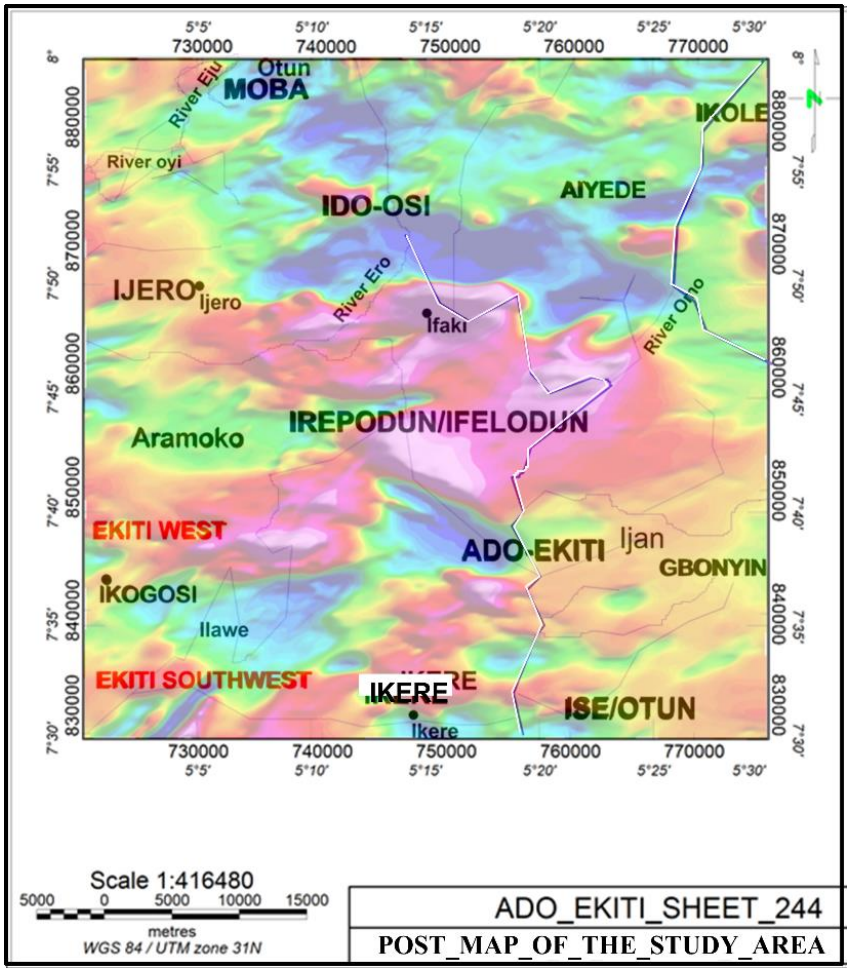

Fig. 4: Post Map of the study area showing localities, drainage patterns, and how the magnetic intensities of various rocks vary from place to place.

The Residual image (Fig. 5) produced a clearer view after the effect of the regional field that obscured the anomalies of interest was removed. On comparison with the TMI and RTE images (Figs. 2 and 3), shallow anomalies with respect to their sources are well defined in the Residual map. The portion delineated in "white" consist of granitic intrusive rocks within migmatite gneises around Ijan, Gbonyin and Ise/Otun while the point marked "D" comprises of the schist of Ijero and quartzite schist of Aramoko. The two flanks are magnetically quiet zones and rich in felsic minerals such as quartz because of their low magnetic character. The areas marked G – G', H – H', J – J', K – K' are parts of the prominent faults tending NE–SW. Other related structures such as dykes and elongated folds are responsible for the anomalies marked E that became widened as of result of intense geological processes such as fracturing and weathering. Although, the identified anomalies (E) were also enhanced by low rich magnetic bearing minerals with infiltrated fluid that differentiated them from areas marked "A" (pink colour).

The Regional field over the study area as calculated from the geomagnetic components is 33200 nT with a likely variation of 26.53 nT/yr, and the regional trend for the basement rocks is NW-SE direction.

Automatic gain control (AGC) (Fig. 6) shows coherent assemblages and alignment of anomalies that appeared characterless in TMI and RTE images by emphasizing equal signals with both low and high amplitude's anomalies that mapped out the structures in the areas. The folds and faults within the entire study area are well delineated and accentuated to unaided eyes and even when compared to other discussed images. The anomalous zones are marked with signals of about 350-472.9 nT and -596 to -400 nT for both positive and negative anomalies respectively, and these areas are the most structurally dominated parts.

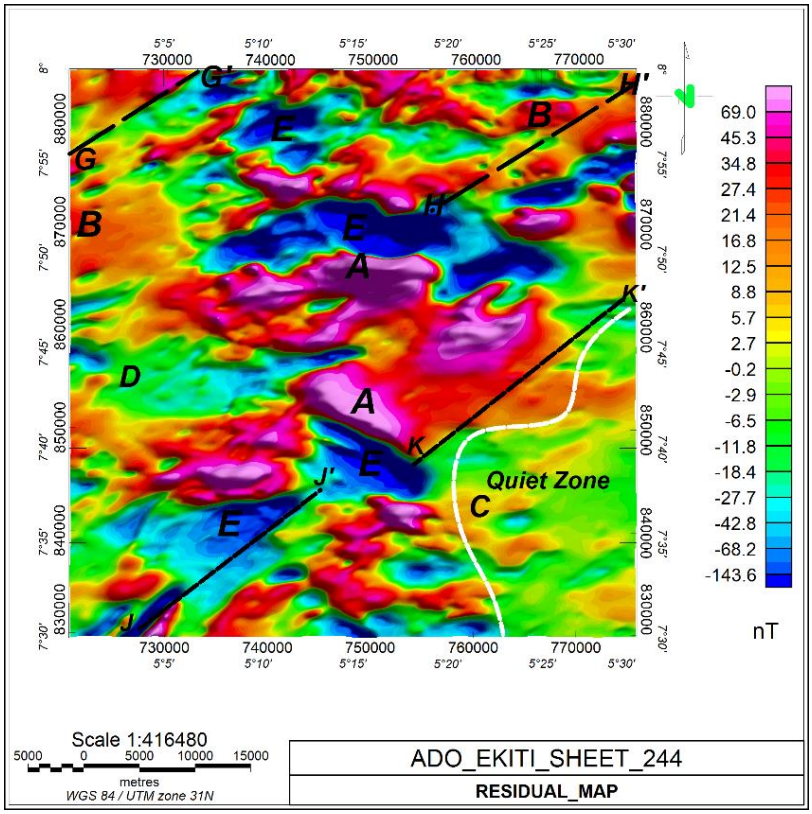

Fig. 5: Residual Map Produced from the Removal of the Regional Field from Total Observed Magnetic Intensity.

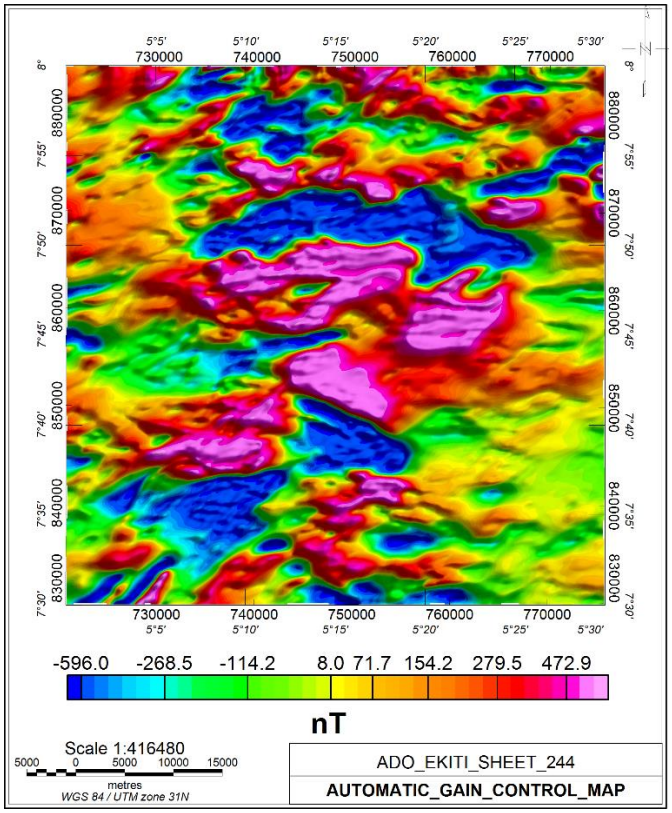

Fig. 6: Automatic Gain Control (Agc) Map.

The downward continuation image (Fig. 7) was produced from RTE data continued downward to 100 m depth after several attempts of using assumed depth of 1000 m and 500 m for the filter, but the filter behaved erratically for these two assumed depths. The downward continuation image accentuates and sharpens the anomalies associated with shallow seated features in the areas.

On the other hand, Figs. 8 (a, b, and c) are the upward continuation images produced by upwardly continuing the RTE data to 1 km (Fig. 8a), 2 km (Fig. 8b) and 3 km (Fig. 8c) respectively to accentuate the responses from basement rocks/deep-seated features.

Comparing the downward and upward continuation images, the downward continued image showed that both positive and negative anomalies are not well pronounced at the surface unlike

when upward continued to a greater depth. However, the upward continued images produced noticeable changes as depth of continuation increases by reducing ambiguities related to delineating the regional and other structures' trends. The upward continued images revealed that the regional trend of the study area is NW-SE, while the fractures (lineaments and faults) trend NE-SW. Some of the negative anomalies at the northern and southwestern parts appear to be less than 2-3 km in depth, but the central positive and negative anomalies with its southwest extension are clearly seen at these depths and far beyond. The continued images revealed that the rocks from the southwestern end trending NNE direction up to the extreme end of northern part have witnessed the highest degree of metamorphism that resulted into high fracturing density, intense weathering and giving ways for minor intrusions to form.

The analytic signal (AS) (Fig. 9) centers the peak of the magnetizing bodies symmetrically over their sources through transformation of the shapes of inclined magnetizing bodies. Consequently, the analytic signal filter was able to accentuate and confine all bodies with the same geometry - A and B on same border line position, while E for the two delineated boundaries of low amplitude signals (yellow lines).

On comparison with Figs. 2, 3, and 5, the highly peaked amplitude areas (A and B) with a reverse Z-like shape signify migmatitic rocks and the edges of magnetizing bodies like basic intrusive and structures. The parts delineated in a “yellow (E)” on border end of high-amplitude signals are the low amplitude signal areas indicating magnetically quiet zones, which are rocks rich in felsic minerals. The image also shows the trend of these bodies as NW-SE for dykes and NE-WS for lineaments and faults.

Horizontal gradient (HG) (Fig. 10) was produced to reveal the anomaly trends of the magnetizing bodies and structural features. The boundaries/faults on horizontal gradient images are usually located at the maxima. There are two possible ways of interpreting the maxima value; one is to correlate with the edge of the mountain body or intrusive of rock, and the other is to correlate with the fault structures (Setyawan et al., 2015). The image shows robust elongated lineaments and other minor fault trends that were not clearly mapped on other images. On comparison, the negative amplitudes in Fig. 10 are well correlated with the shape of the highly peaked areas (A and B) in Fig. 9; this further established the nature of rocks and structural evolution (structures and trends) in the study area.

The Shaded Relief image of the study area (Fig. 11) shows the overall distribution of the surface to subsurface topography of the magnetized bodies. Regions A, B and C are delineated and classified based on the degree of ruggedness of the study area. The potions B and C within two border lines (yellow) are highly rugged compared to Regions A due to high level of fracturing and weathering. Depths of both the positive and negative anomalies were determined relatively to their positions. Areas identified as A and B had depth range of about 1.4 km being the upper layers than areas marked C which is 0.4 km at lower depth (having a total depth of about 1.8 km). Note that these depths are to the top of the magnetizing bodies and not the entire depth profiles of the basement rocks in the study area. Furthermore, the image reveals the trends of the lineaments are in NE-SW, NNE-SSW and approximately N-S directions, and intrusive dykes are in NW-SE, NNW-SSW directions (both in green colour), though there are some minor lineaments in E-W direction.

Radially Averaged Power Spectrum (RAPS) (Fig. 12) showed the total depth estimate to the top of magnetic sources that produced the observed anomalies in the study area using spectral analysis. The gradient of the layers were calculated based on the wavelength of the magnetic sources. The gradients are: shallower layer (-0.25) and deeper layer (-22.7) with an approximate depth estimates of 0.02 km and 1.80 km respectively. The total depth estimates from the centre grid ranges from shallower sources (20 m) to deeper sources (1.8 km). Therefore, both the surface relief and spectral plot filters can be used for depth to top of magnetic source estimate because of their abilities to show differences in depth for shallower and deeper magnetizing bodies.

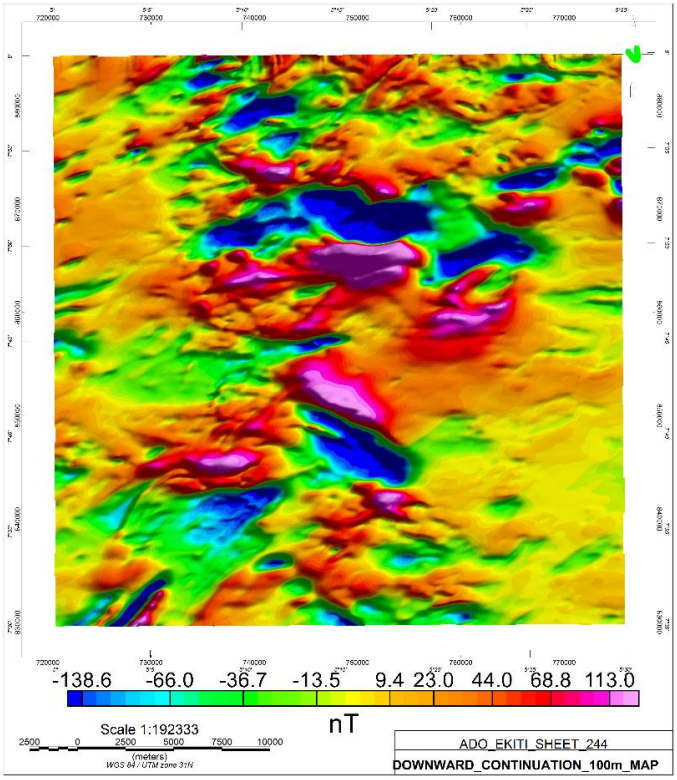

Fig. 7: Downward Continuation Map.

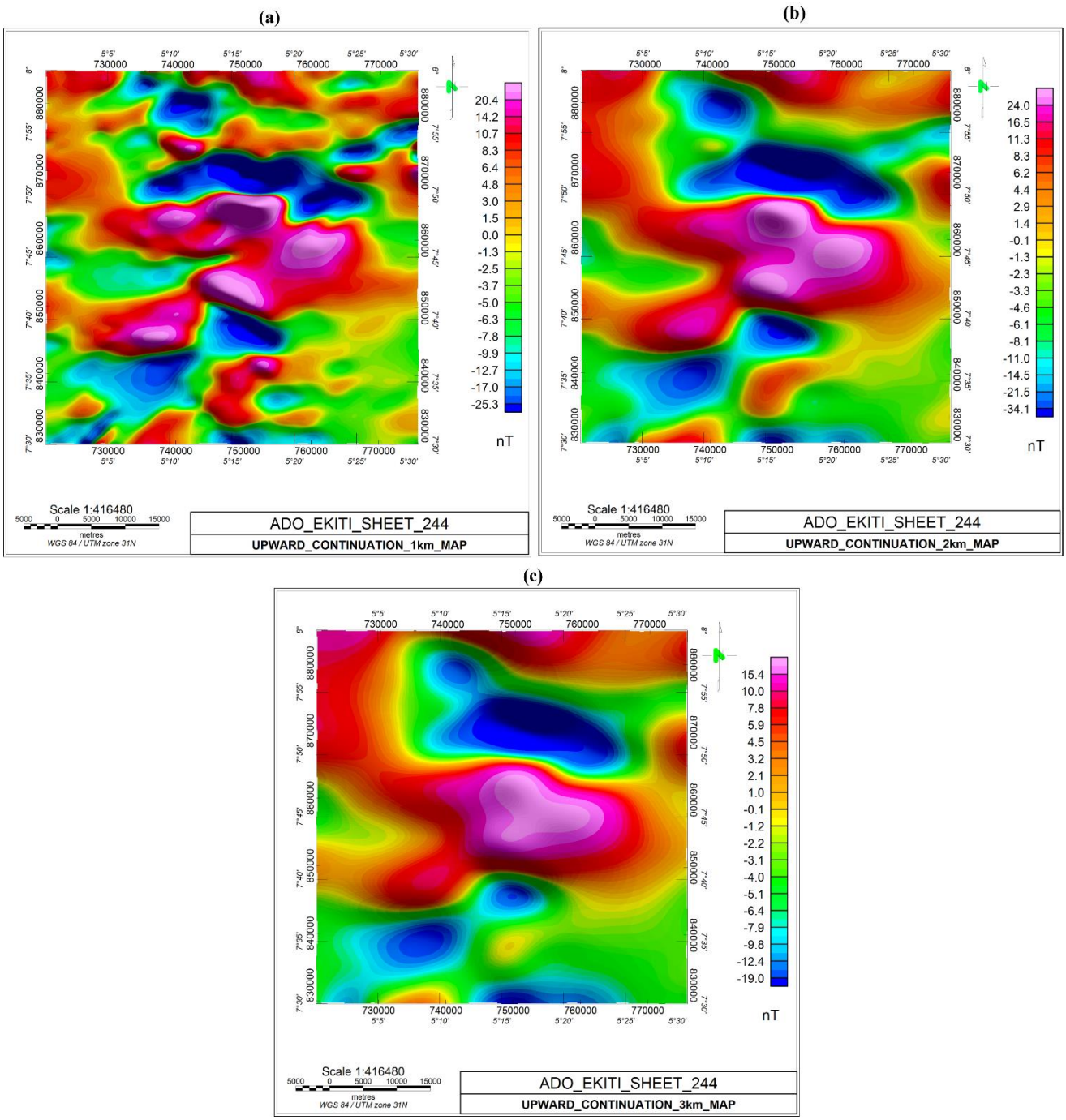

Figs. 8: Upward Continuation Maps, at; (A) 1km, (B) 2km and (C) 3km.

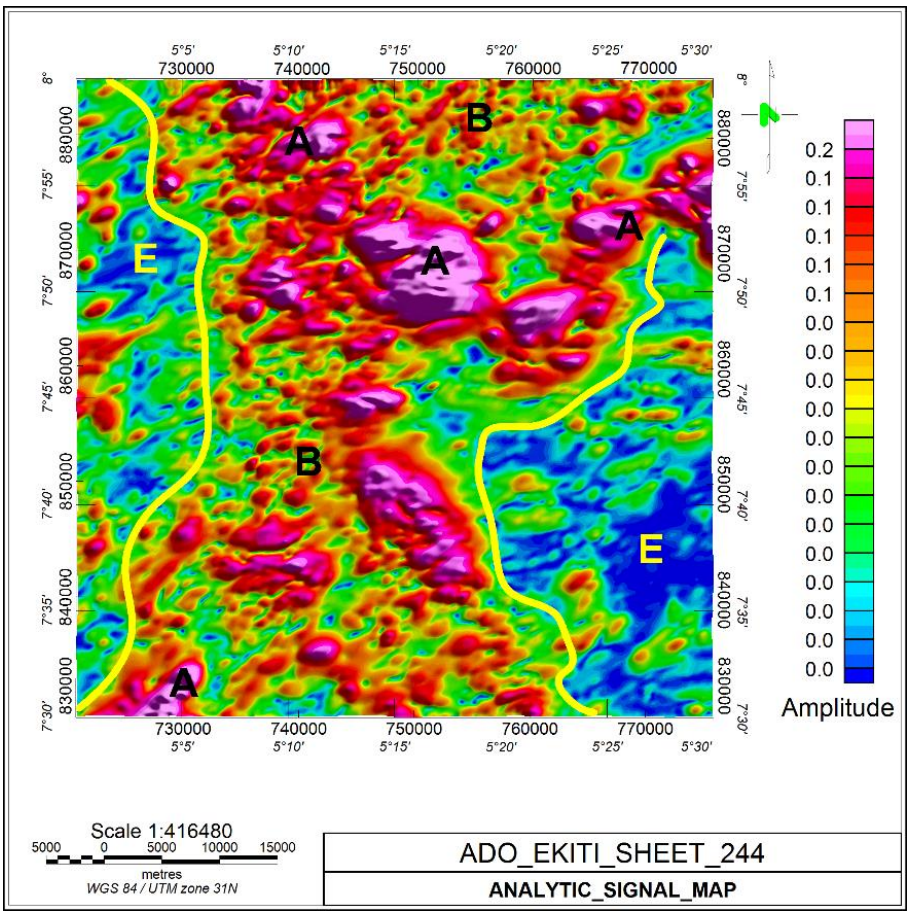

Fig. 9: Colour Shaded Analytic Signal (AS) Map.

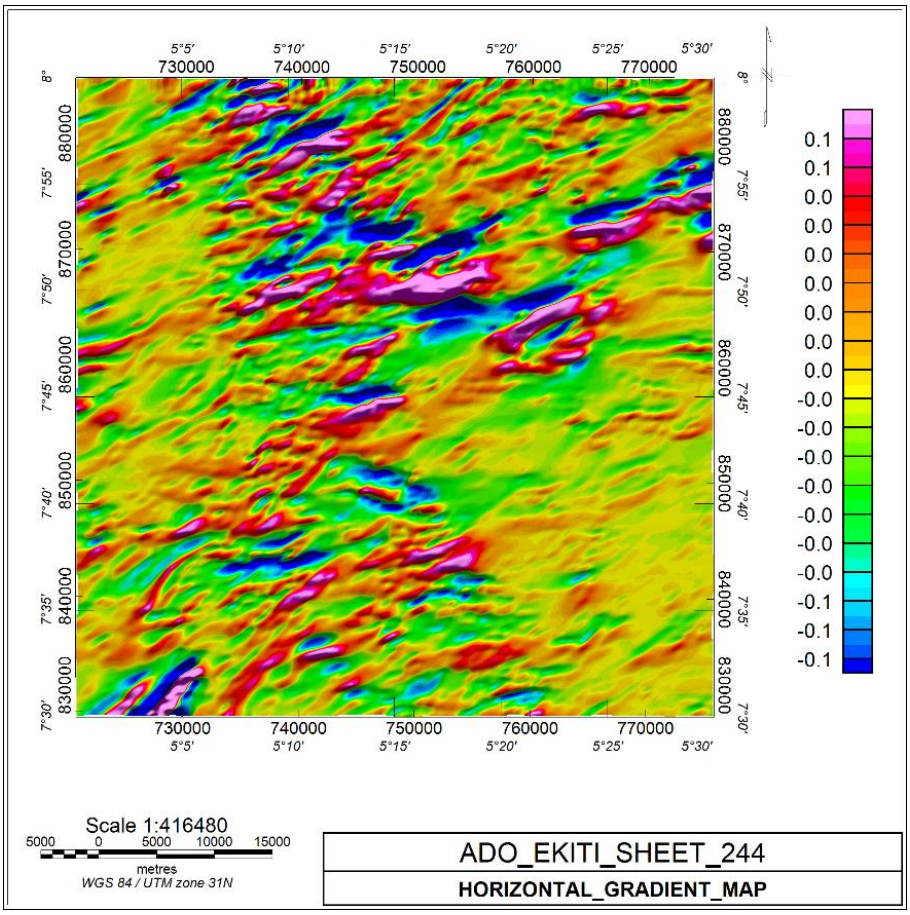

Fig. 10: Horizontal Gradient (HG) Map of the Study Area.

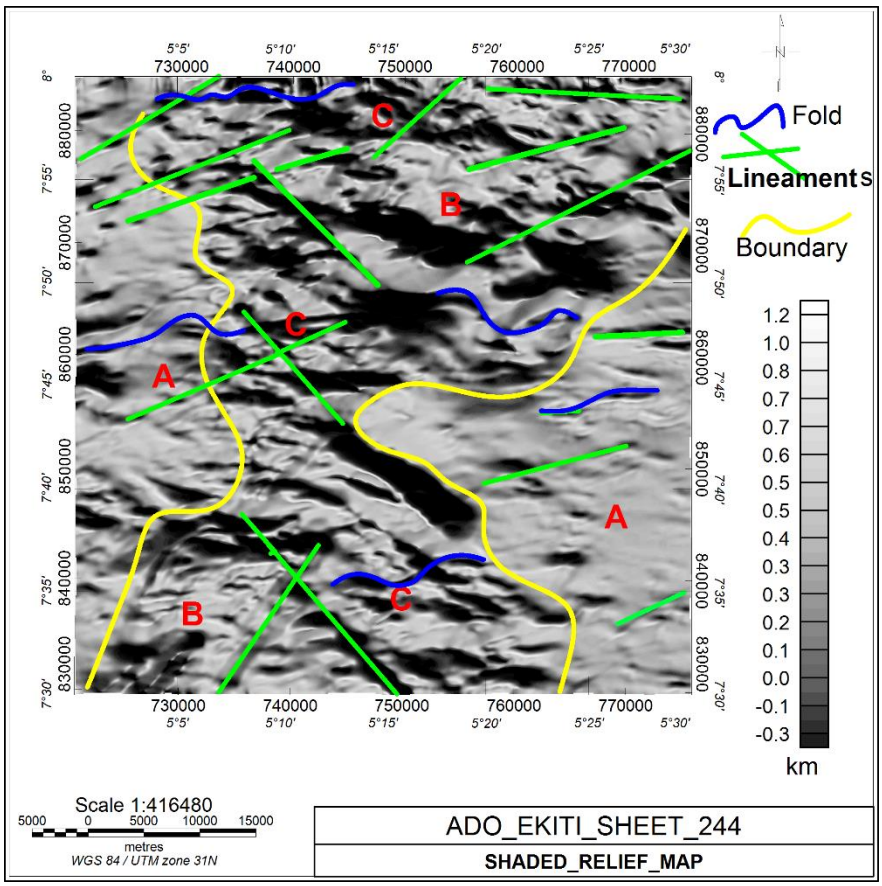

Fig. 11: Shaded Relief Map of the Study Area.

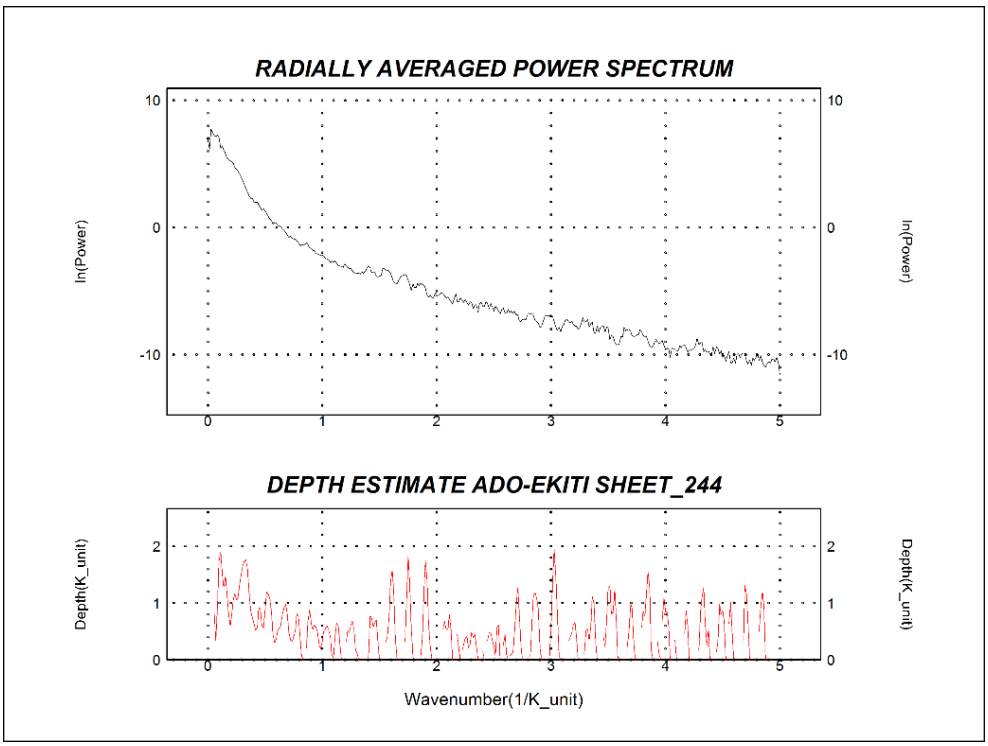

Fig. 12: Radially Averaged Power Spectrum (RAPS)/Spectral plot for Estimating Depth to Magnetic Sources.

5. Conclusion

Classification of the basement and structures by using all the available results from processed aeromagnetic data of Ado-Ekiti area has proven the robustness and worthiness of using enhanced magnetic data reduction in mapping and delineating basement rocks, regional and structural trends, anomaly closures, and depth estimate of magnetizing bodies.

The positive anomalies were identified to have resulted from highly rich magnetic bearing-minerals present in the rocks, well arranged crystal lattice frameworks, fewer deformations (structures) and their closeness to the surface. On the other hand, the negative anomalies have resulted from rocks that have low

ferromagnetism minerals and from highly deformed rocks with diverse structures such as lineaments and faults trending NE-SW, NNE-SSW, E-W (minor) and approximately N-S directions and intrusive dykes, which are in NW-SE, NNW-SSW directions. The negative anomalies could also be attributed to intense weathering and infiltrated fluids through shear zones (faults and joints) and low rich magnetic bearing-minerals serving as infill within the weathered basement rocks.

The results of Figs. 2, 3, 5 and the analytic signal have also evinced that the complexes have been highly deformed and weathered, due to actions of metamorphism and metasomatism that restructured these rocks through folding, fracturing, alterations of mineralogical compositions, deformation of crystal lattices, etc. These processes resulted into formation of geological structures and intrusives like dykes seen within and around the study area.

The delineated structures will play a vital role in mineral and groundwater explorations because they usually serve as host for minerals and channels for groundwater accumulation respectively. However, the impacts of these structures on engineering constructions such as roads, super-structures (building), dams, etc. and in environmental studies cannot be boycotted. The deep–seated faults could cause foundation failure if reinforced/pilling concretes were not used. Also, they could serve as passage ways for leachates to migrate if dumpsites/landfill were sited in such areas. Proper measures must be taken while siting such, because some of these faults are at near-surface depth.

Hence, detailed ground survey is recommended to further classify the delineated areas to ascertain the type of minerals within these structures and also areas that will be suitable for high groundwater yield, high rise buildings and siting of dumpsites/landfills.

References

[1] Abraham, E. M., Lawal, K. M., Ekwe, A. C., Alile, O., Murana, K. A. and Lawal, A. A. (2014). Spectral analysis of aeromagnetic data for geothermal energy investigation of Ikogosi Warm Spring - Ekiti State, Southwestern Nigeria. *Geothermal Energy, Springer Open Journal*, vol. 26, pp. 1-21. https://www.geothermal-energy-journal.com/content/2/1/6.

[2] Ademilua, O. L. (1997). A Geoelectric and Geologic Evaluation of Groundwater Potential of Ekiti and Ondo States, Southwestern Nigeria, Unpublished M.Sc. Thesis, Department of Geology, Obafemi Awolowo University, Ile-Ife, Nigeria. pp. 1-67.

[3] Ajibade, A. C., and Fitches W. R. (1988). The Nigerian Precambrian and the Pan–African Orogeny. Precambrian Geology of Nigeria. pp. 45-53.

[4] Ansari, A. H. and Alamdar, K. (2009). Reduction to the Pole of Magnetic Anomalies Using Analytic Signal. *World Applied Sciences Journal*, vol. 7(4), pp. 405-409.

[5] Ayodele, O. S. (2013). Geology and Structure of the Precambrian Rocks in Iworoko, Are, and Afao Area, Southwestern, Nigeria. *International Research Journal of Natural Sciences*, vol. 1, no. 1, pp. 14 – 29.

[6] Bayowa, O. G., Olorunfemi, O. M., Akinluyi, O.F. and Ademilua, O. L. (2014). A Preliminary Approach to Groundwater Potential Appraisal of Ekiti State, Southwestern Nigeria. *International Journal of Science and Technology*, vol. 4, no. 3. pp. 48-58.

[7] Briggs I. C., (1974). Machine contouring using minimum curvature. *Geophysics*, vol. 39, pp. 39-48. https://doi.org/10.1190/1.1440410.

[8] Eze, C. L., Sunday, V. N., Ugwu, S. A., Uko, E. D., Ngah, S. A. (2011). Mechanical model for Nigerian intraplate earth tremors. Earthzine. http://www.earthzine.org/2011/05/17/mechanical-model-for-nigerian-intraplate-earth-tremors

[9] Fitzgerald, D., Yassi, N. and Dart, P. (1997). A case study on geophysical gridding techniques: INTREPID perspective. *Exploration Geophysics*, vol. 28, pp. 204-208. https://doi.org/10.1071/EG997204.

[10] Gunn, P., Maidment, D. and Milligan, P. (1997). Interpreting aeromagnetic data in areas of limited outcrop. *AGSO Journal of Australian Geology and Geophysics*, vol. 17, no. 2, pp. 175–185.

[11] Hsu, S., Sibuet J. C. and Shyu, C. (1996). High-resolution detection of geologic boundaries from potential field anomalies: an enhanced analytic signal technique. *Geophysics*, vol. 61, pp. 373-386. https://doi.org/10.1190/1.1443966.

[12] Hsu, S., Sibuet J. C. and Shyu, C. (1998). Depth to magnetic source using the generalized analytic signal. *Geophysics*, vol. 63, pp. 1947-1957. https://doi.org/10.1190/1.1444488.

[13] Jeng, Y., Lee, Y. L., Chen, C. Y. and Lin, M. J. (2003). Integrated signal enhancements in magnetic investigation in archaeology. *Journal of Applied Geophysics*, vol. 53, pp. 31–48. http://dx.doi.org/10.1016/S0926-9851.

[14] Jones, H. A. and Hockey, (1964). The Geology of part of' Southwestern Nigeria. Nigerian Geological Survey, bulletin No, 31.

[15] Leu, L. K. (1981). Use of reduction-to-equator process for magnetic data interpretation. Presented at the 51st Ann. Internat. Mtg., Sot. Exnl. Geonhv. *Geophysics*, vol. 47, pp. 445.

[16] Luyendyk, A. P. J. (1997). Processing of airborne magnetic data. *AGSO Journal of Geology and Geophysics*, vol. 17, pp. 31-38.

[17] Mackey, T., Lawrie, K. Wilkes, P., Munday, T., de Souza K. N., Chan, R., Gibson, D., Chartres, C. and Evans, R. (2000). Paleochannels near West Wyalong, New South Wales: A case study in delineation and modelling using aeromagnetics. *Exploration Geophysics*, vol. 31, pp. 1-7. https://doi.org/10.1071/EG00001.

[18] MacLeod, I. N., Jones, K. and Ting Fan Dai, (1993). 3-D analytic signal in the interpretation of total magnetic field data at low magnetic latitudes. *Exploration Geophysics*, vol. 24, pp. 679-688. https://doi.org/10.1071/EG993679.

[19] Milligan, P. R. and Gunn, P. J. (1997). Enhancement and presentation of airborne geophysical data. *AGSO Journal of Geology and Geophysics*, vol. 17, pp. 63-75.

[20] Montaj™, (2004). Tutorial and help file on Two–Dimensional frequency domain processing of potential field data.

[21] Mudge, S. T. (1991). New developments in resolving detail in aeromagnetic data. *Exploration Geophysics*, vol. 22, pp. 277-284. https://doi.org/10.1071/EG991277.

[22] Nabighian, M. N. (1972). The analytic signal of two-dimensional magnetic bodies with polygonal cross-section: its properties and use for automated anomaly interpretation. *Geophysics*, vol. 37, pp. 501–517. https://doi.org/10.1190/1.1440276.

[23] Okpoli, C. and Akingboye, A. (2016a). Reconstruction and appraisal of Akunu–Akoko area iron ore deposits using geological and magnetic approaches.*RMZ – Materials and Geoenvironment Journal*, vol. 63. pp. 19-38.

[24] Okpoli, C. C. and Akingboye, A. S. (2016b). Magnetic, radiometric and geochemical survey of quarry sites in Ondo State, Southwestern Nigeria. *International Basic and Applied Research Journal*, vol. 2, no. 8, pp. 16-30.

[25] Okubo, Y., Matsushima, J., Correia, A. (2003). Magnetic spectral analysis in Portugal and its adjacent seas. *Physics and Chemistry of the Earth*, vol. 28, pp. 511–519. https://doi.org/10.1016/S1474-7065(03)00070-6.

[26] Okunlola, A. O., Akinola, O. O. and Olorunfemi, A. O. (2011). Petrochemical Characteristics and Industrial Features of Talcose Rock on Ijero Area, Southwestern Nigeria. *Ife Journal of Science*,vol. 13, no. 2, pp. 317 – 326.

[27] Oladapo, M. I. and Ayeni, O. G. (2013). Hydrogeophysical Investigation in Selected Parts of Irepodun/Ifelodun Local Government Area of Ekiti State, Southwestern Nigeria. *Journal of Geology and Mining Research*, vol. 5, no. 7, pp. 200 – 207. https://doi.org/10.5897/JGMR2013.0183.

[28] Oluyide, P. O., Udoh, A. N. (1989). Preliminary comments on the fracture systems of Nigeria. In: Ajakaiye, D. E., Ojo, S. B. and Daniyan M. A. (ed.)Proceedings of the national seminar on earthquakes in Nigeria. pp. 97–109.

[29] Omosanya, K. O., Ariyo, S. O., Kaigama, U., Mosuro, G. O., and Laniyan, T. A. (2015). An outcrop evidence for polycyclic orogenies in the basement complex of Southwestern Nigeria. *Journal of Geography and Geology*, vol. 7, no. 3, pp. 24-34. https://doi.org/10.5539/jgg.v7n3p24.

[30] Oyinloye, A. O. (2011). Geology and Geotectonic Setting of the Basement Complex Rocks in Southwestern Nigeria: implications

on Provenance and Evolution. *Earth and Environmental Sciences*, pp. 98 – 117.

[31] Rahaman, M. A. (1976). Review of Basement Geology of Southwestern Nigeria. In: Kogbe, C.A., (ed.) *Geology of Nigeria.* Rock View (Nig.) Limited, Jos, Nigeria. pp. 39-56.

[32] Rahaman, M. A. (1981). Recent Advances in the Study of the Basement Complex of Nigeria. First Symposium on the Precambrian Geology of Nigeria, Summary.

[33] Rahaman, M. A., Emofureta, W. O. and Vachette, M. (1983). The potassic-granites of the Igbeti area: further evidences of the polycyclic evolution of the Pan-African belt in Southwestern Nigeria. *Precambrian Res*., 22, pp. 75-92. https://doi.org/10.1016/0301-9268(83)90059-1.

[34] Rajagopalan, S. (1987). The use of automatic gain control to display vertical magnetic gradient data. *Exploration Geophysics*, vol. 18, pp. 166-169. https://doi.org/10.1071/EG987166.

[35] Rajagopalan, S. and Milligan, P. (1995). Image enhancement of aeromagnetic data using automatic gain control. *Exploration Geophysics*, vol. 25, pp. 173-178. https://doi.org/10.1071/EG994173.

[36] Roest, W. R., Verhoef, J. and Pilkington, M. (1992). Magnetic Interpretation using the 3D Analytic Signal, *Geophysics*, vol. 57, pp. 116-125. https://doi.org/10.1190/1.1443174.

[37] Ross, C. B. (2000). Airborne and Ground Magnetics. In: Papp, E. (ed.) Geophysical and Remote Sensing Methods for Regolith Exploration, CRCLEME Open File Report 144. pp. 33-45.

[38] Salem, A., Williams, S., Fairhead, J., Ravat, D. and Smith, R. (2007). Tilt-depth method: a simple depth estimation method using first-order magnetic derivatives. *The Leading Edge*, vol. 26, pp. 1502-1505. https://doi.org/10.1190/1.2821934.

[39] Setyawan, A., Yudianto, H., Nishijima, J. and Hakim, S. (2015). Horizontal Gradient Analysis for Gravity and Magnetic Data beneath Gedongsongo Geothermal Manifestations, Ungaran, Indonesia. Proceedings World Geothermal Congress, Melbourne, Australia. pp. 1-6.

[40] Telford, W. M., Geldart, L. P., Sheriff, R. E., Keys, D. A. (1990). *Applied Geophysics*. Cambridge University Press. https://doi.org/10.1017/CBO9781139167932.

[41] Woakes, M., Ajibade, C. A., and Rahaman, M. A. (1987). Some metallogenic features of the Nigerian Basement. *Journal of Africa Science*, vol. 5, pp. 655-664.